Surfactant Chromatographic Movement: An Experimental Study

J. H. HARWELL
R. S. SCHECHTER
and W. H. WADE

University of Texas at Austin
Department of Chemical Engineering
Austin, TX 78712

Previous papers (Trogus et al., 1979a; Harwell et al., 1982) have developed a theory of surfactant chromatographic movement on the assumption that micelles may be treated as a separate thermodynamic phase in predicting surfactant adsorption. The work examined here demonstrates that, even with incorporation of the complex surface interactions between surfactant molecules that are present in real systems, conclusions and observations made in the previous studies hold true. Additionally, theoretical predictions are compared to experimental results to demonstrate that for the system studied the phase separation model of micelle formation (Shinoda, 1963) and the plateau adsorption model (Trogus et al., 1979a) are powerful and useful simplifications for predicting surfactant chromatographic behavior.

SCOPE

Enhanced oil recovery processes that use surfactants to decrease the interfacial tension between oil and water to a level low enough to release oil drops trapped within porous media by capillary forces have now been tested extensively in the laboratory and to a lesser extent in actual field trials (Lake and Pope, 1979). The technology has improved rapidly, and commercial application now appears feasible (Holm, 1982). One potential difficulty of major concern is related to the chromatographic separation of the surfactant molecules that comprise the total surfactant system. All commercial surfactants that are candidates for oil recovery agents are mixtures of different molecules, and since the surfactant solution must flow through a porous bed of minerals to reach the trapped oil drops, some chromatographic separation is inevitable.

In previous papers (Trogus et al., 1979a; Harwell et al., 1982), the theory of surfactant chromatographic separation has been presented and some surprising predictions have emerged from this work. The essential feature of surfactant behavior that distinguishes it from the usual events that take place when interacting components are introduced into a chromatographic column (Aris and Amundson, 1973; Helfferich and Klein, 1970) is the fact that surfactants aggregate together in aqueous solution to form mixed micelles. These mixed micelles, which contain representatives of all of the molecules in solution, are in equilibrium with surfactant monomer (unaggregated surfactant molecules), which, in turn, are in equilibrium with surfactant adsorbed on the surface. Different proportions of the surfactant molecules will appear in the micellar, monomer, and adsorbed states (Trogus et al., 1979b). It is this difference that makes the surfactant chromatographic separation different from other interacting systems.

Based on a greatly simplified model of adsorption (Trogus et al., 1979b) that assumes a Henry law adsorption relationship between surfactant monomer and the adsorbed surfactant and that considers the micelles to be a separate thermodynamic phase (the so-called pseudo phase separation model; Shinoda, 1963) Harwell et al. (1982) have reported several important features of the chromatographic separation of micellar solutions. One of the most striking was the discovery of *indifferent concentration waves* that move with the fluid velocity, indicating no interaction with the substrate. The conditions for the existence of such waves were shown to be quite general. Other interesting phenomena such as surfactant concentration overshoot and the possibility of the more strongly adsorbed surfactant molecules advancing through the column more rapidly than those that are less strongly adsorbed have also been predicted.

The purpose of this paper is to present for the first time experimental evidence demonstrating almost all of the predicted behavior. The prediction that the more strongly adsorbed molecule could, under some circumstances, advance more rapidly than others was based on a theory that neglects diffusion; results reported here demonstrate that at least for the system studied even an infinitesmal diffusive flux will "destroy" the mathematical solution of the coupled set of hyperbolic equations and lead to an entirely different mode of chromatographic transport that tends to resist separation. This is the only example known to the authors for which a small diffusive perturbation will modify the solution of the diffusionless mass conservation in a discontinuous fashion.

The experimental results also exhibit new features of the effluent histories not heretofore known to exist. These new features arise primarily because surfactant molecules tend to aggregate on the surface of the solid as well as in solution. There is a distinct solution concentration at which surface aggregates first form; in this paper, that concentration is called the critical admicelle concentration (CAC).

CONCLUSIONS AND SIGNIFICANCE

This paper examines the effects of the interactions of adsorption, mixed micelle formation, and dispersion on the chromatographic movement of surfactant mixtures. Results presented here demonstrate conclusively that the plateau adsorption model of surfactant adsorption and the phase separation model of micelle formation are, if not exact, very powerful concepts for understanding surfactant adsorption and chro-

J. H. Harwell is currently at The University of Oklahoma, Department of Chemical Engineering and Materials Science, Norman, OK 73069.
Correspondence concerning this paper should be addressed to R. S. Schechter.

matographic movement. Not only are these results important to the modeling of the chromatographic movement of surfactant mixtures, but they are also important to resolving the issue of the explanation of the low concentration adsorption maximum observed in many surfactant systems; this maximum has been explained as a result of reductions in chemical potential of surfactants in the system from changes in the composition of the micelles with increasing surfactant concentration (Trogus et al., 1979b) and by electrostatic exclusion of micelles from the solid/solution interface (Ananthapadmanabhan and Somasundaran, 1983), among others. Predictions based on assuming the phase separation model and the plateau adsorption model are shown in the results that follow to be observable in real systems; that these models are reasonable approximations for the systems studied here gives strong credence to the use of these models to explain the low concentration adsorption maximum.

For a more immediately practical point of view, several aspects of surfactant chromatographic movement that have potentially significant implications for enhanced oil recovery chemical flooding have been pointed out. Our experimental results have borne out earlier predictions regarding the existence of a unit velocity wave that forms at the rear of the surfactant slug. This fast-moving wave will tend to overtake the front of the slug, reducing its oil recovery effectiveness.

Also reported for the first time is the existence of a low concentration surfactant wave, corresponding to the CAC, which moves rapidly through the porous medium, accounting for the heretofore unexpected early breakthrough of surfactant observed in field tests of micellar-polymer-enhanced oil recovery processes (Holm, 1982; Aho and Bush, 1982).

SURFACTANT ADSORPTION

Understanding the mechanisms of surfactant chromatography forms the main thrust of this work. Chromatographic separation is, however, intimately related to adsorption, and it is therefore necessary to consider multicomponent surfactant adsorption. The basic concepts have been described by Scamehorn et al. (1982a, 1982b) and extended by Harwell (1983). The details of the adsorption model and its mathematical development are far too complex to be included here, but the fundamental concept is simple: Total surfactant adsorption is composed of the sum of adsorption on local surface patches (see Scamehorn, 1982a); adsorption on a local patch on the surface is given either by a Henry's law coefficient when the coverage on that patch is low or by complete bilayer coverage obtained at a critical admicelle concentration. Figure 1 depicts the adsorption of an isomerically pure surfactant as modeled. In region I, where the surfactant solution concentration is small, individual molecules are adsorbed. In region II the first bilayer structure forms on the most energetic surface patch. As the solution composition is increased, the fraction of the surface covered with a bilayer is shown (region III) to have correspondingly increased.

In a monoisomeric surfactant system, when micelles form in solution, adsorption ceases and a plateau is reached. Further increases in surfactant concentration only serve to increase the number of micelles.

The picture is much more complex when the surfactant system is a multicomponent one. The Henry's law constant for a local patch on the surface is a function of the surfactant structure, and the bilayered surfactant aggregates at the solid/solution interface (called admicelles in this paper) contain all surfactant species just as micelles do. A mathematical description of all of these mechanisms has been developed (Harwell, 1983) and will be published elsewhere. For our purposes some insight is required to understand the results, but seeing the details of the model is not crucial.

The surfactants used in this study were synthesized by Dr. El-Emary using techniques that have been reported (Doe et al., 1977). Their structures, names, and abbreviations used in this work appear in Figure 2. The substrate used was a low surface area, nonporous α-alumina that was selected to minimize nonequilibrium effects

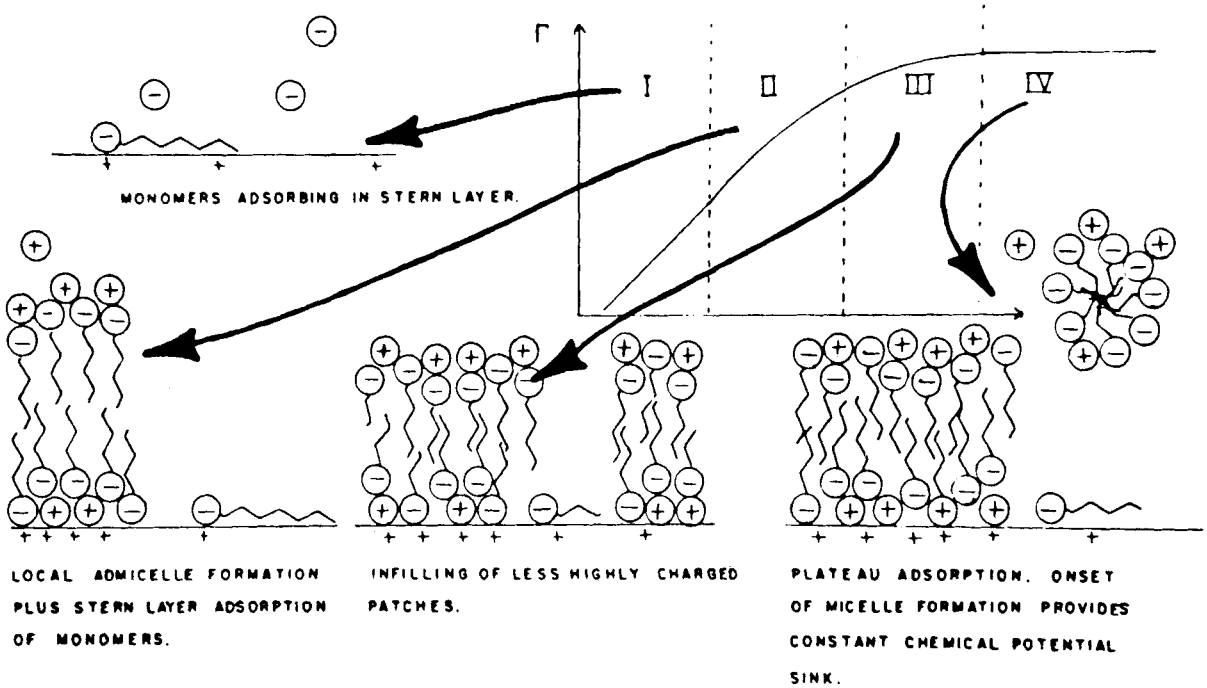

Figure 1. Schematic presentation of the admicelle hypothesis of surfactant adsorption.

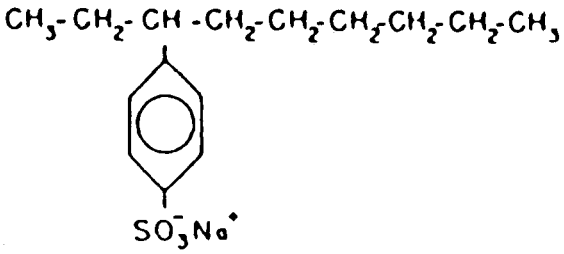

Sodium P(1-butyl heptyl) Benzene Sulfonate
(3-ϕ-C_9 ABS)

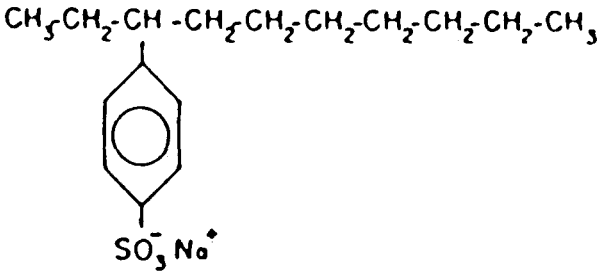

Sodium P(1- butyloctal) Benzene Sulfonate
(3-ϕ-C_{10} ABS)

Figure 2. Surfactants, names, and abbreviations used in this study.

due to pore diffusion. Experimental details are reported elsewhere (Harwell, 1983).

Experimental pure component isotherms are shown in Figures 3 and 4. These isotherms display the characteristic shape depicted by Figure 1. The linear portion at low concentrations corresponds to the Henry's law region, and the CAC marks the sharp transition shown between regions I and II.

The concentration at which the adsorption plateau begins is slightly in excess of the surfactant CMC as determined from surface tension measurements. To emphasize this point, the dashed line

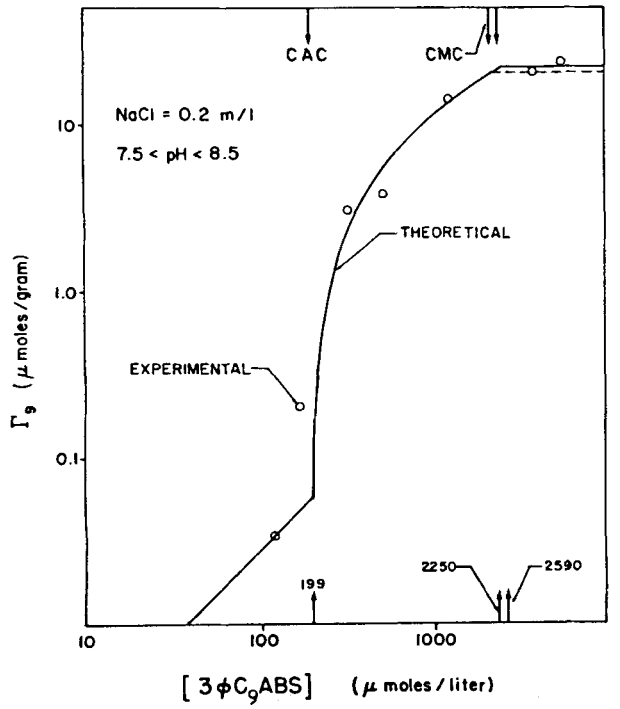

Figure 3. Experimental and theoretical adsorption of 3ϕC_9ABS on α-alumina.

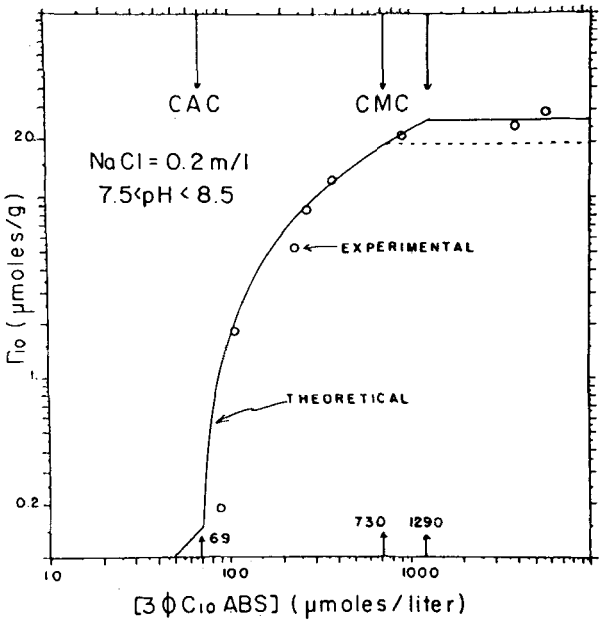

Figure 4. Experimental and theoretical adsorption of 3ϕC_{10}ABS on α-alumina.

in Figures 3 and 4 represents the predicted plateau adsorption based on the CMC. It is seen that this value is less than the measured plateau adsorption. This discrepancy is thought to be attributable to the inherent inaccuracy of the phase separation model near the CMC. Micelles form over a range of concentrations and the chemical potential of surfactant monomer increases sufficiently with increasing surfactant concentration in the region of the CMC to result in measurable adsorption beyond the numerical value of CMC arising from use of the phase separation model.

The adsorption of binary surfactant mixtures has been calculated based on the pure component data shown in Figures 3 and 4 using a theory recently developed (Harwell, 1983). The predicted total surfactant adsorption as a function of the individual concentrations is shown as a contour plot in Figure 5. The contours of constant total surfactant concentration appear parallel to the CAC curve for the binary mixture. When compared to the experimental results, it can be seen that the predictions are accurate. This is the essential point with regard to this work since the chromatographic calculations

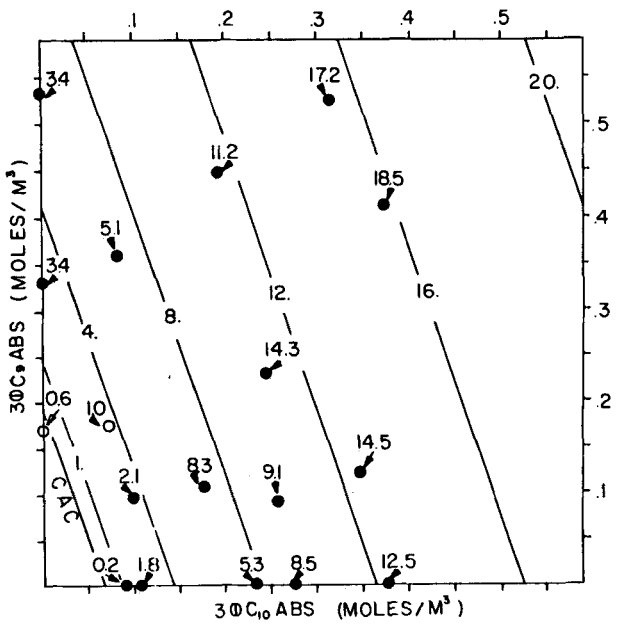

Figure 5. Total surfactant adsorption vs. 3ϕC_9 and 3ϕC_{10} concentration.

require the isotherms as input. Prediction of surfactant adsorption must be correct whether the underlying theory incorporated in the theoretical isotherms is flawed or not; the physical mechanisms incorporated into the adsorption model are irrelevant insofar as the application of the isotherm to chromatographic calculations. If, for example, the local surfactant aggregates are hemimicelles (Somasundaran and Fuerstenau, 1966) rather than admicelles, the predicted chromatographic behavior will not change as long as the *amount* of adsorption and the slope of the isotherm are correct. Because our main goals relate to chromatographic separation, not adsorption, we have not attempted to present any of the arguments used in developing the isotherm. There are however features of the adsorptive process that are important to understand to order for one to be able to interpret the chromatograms. In summary, these are

1. A CAC that depends on the solution composition exists. At this point a sharp increase in adsorption is observed because of the onset of surface aggregate formation. The surface aggregates are mixtures of all surfactant species present in solution.
2. For a binary mixture of surfactants, the CAC appears linear in concentration space (see Figure 5).
3. Bilayered local surfactant aggregates called admicelles form, and their surface coverage increases with increasing solution concentration.
4. For pure component systems an adsorption plateau exists at concentrations slightly in excess of the CMC determined by surface tension measurements. For the binary mixtures studied here, adsorption increases or decreases slightly at mixture concentrations in excess of the mixture CMC owing to mixed micelle behavior, but the isotherm breaks sharply at concentrations slightly in excess of the mixture CMC.

MIXED MICELLES

Micelles are transient aggregates of surfactant monomers, consisting of 10 to 30 molecules that decompose and reform rapidly. Individual surfactant molecules (monomers) are distributed throughout the aqueous phase surrounding the micelles. These can and often do exchange with aggregated molecules. If the surfactant is a mixture, then the individual micelles will be mixed; that is, each will contain surfactant of all types present in the solution. Although the monomer molecules are in equilibrium with the micelles, the composition of surfactant in each of the pseudophases is different. The mathematical treatment of this phenomenon is well known (Shinoda, 1963; Mysels and Otter, 1961), and the method by which it is incorporated into the chromatographic equations has been treated in earlier works (Harwell et al., 1982; Harwell, 1983).

The phase separation model of micelle formation assumes that the chemical potential of surfactant in solution is determined by the concentration of the monomers. The plateau adsorption model assumes that surfactant adsorption is determined by the monomer concentrations; adding micelles of the same composition as those already present in the system does not change the monomer concentrations nor does it affect the adsorption. This is what was meant in earlier papers when the statement was made that "micelles do not adsorb" (Harwell et al., 1982; Trogus et al., 1979a, 1979b). Though the picture this statement was meant to convey has not changed, the statement itself is now being abandoned by the authors, as it is recognized that it leads to confusion as surfactant aggregates that form at the solid/solution interface are very micelle-like in nature and morphology (Harwell, 1983; Scamehorn et al., 1982a; Somasundaran and Fuerstenau, 1966). Previous workers have referred to these local micelle-like surfactant aggregates at the solid/liquid interface as "hemimicelles," but the authors of the present paper prefer the term "admicelles," as these structures may often be bilayered in nature rather than local monolayer structure, as the term "hemimicelle" implies (Scamehorn et al., 1982a; Somasundaran and Fuerstenau, 1966).

Method of Solution

The solution of the above equations is obtained by application of coherence (Helfferich and Klein, 1970) or simple wave theory (Aris and Amundson, 1973), as these two approaches lead to identical solution procedures for the case studied here. This is the same method of solution as that applied in a previous paper (Harwell et al., 1982), which considered chromatographic separation based on idealized, theoretical isotherms. Because the calculation procedure is the same as that previously reported, the

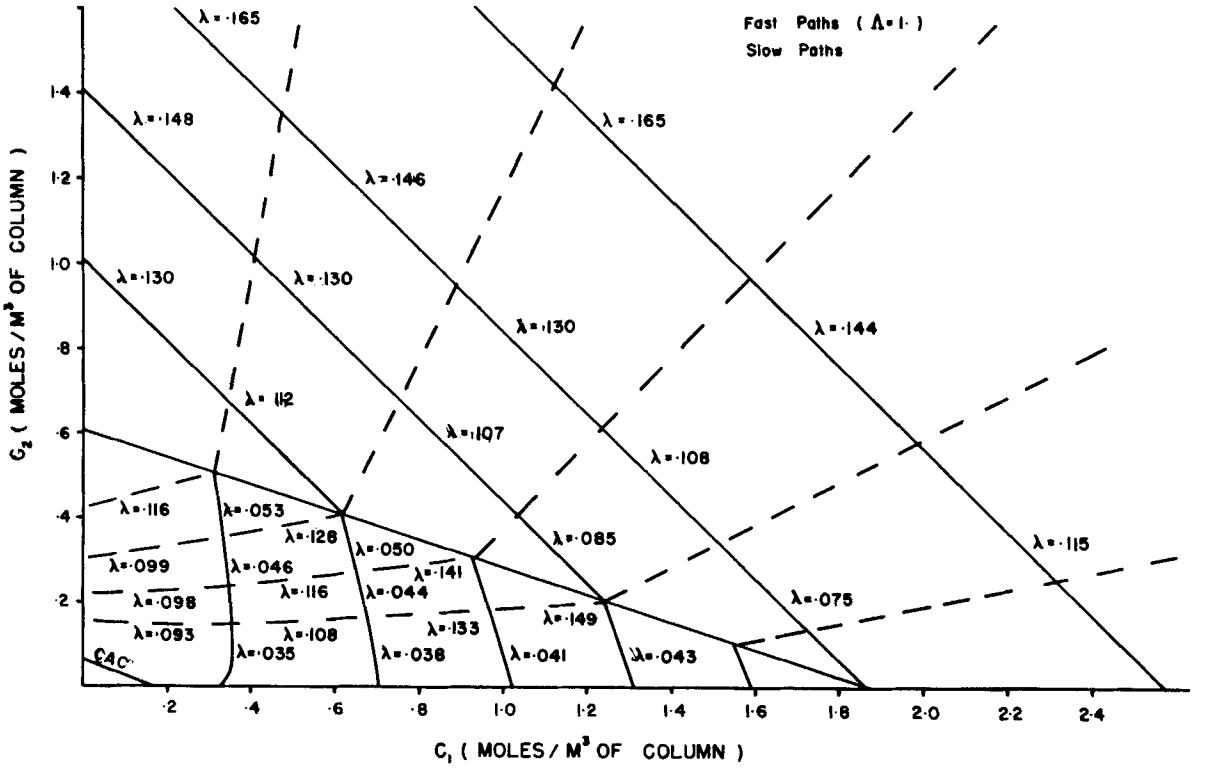

Figure 6. Composition path grid for $3\phi C_9$ABS/$3\phi C_{10}$ABS on α-alumina in 0.2 M NaCl, pH 8, T = 30°C.

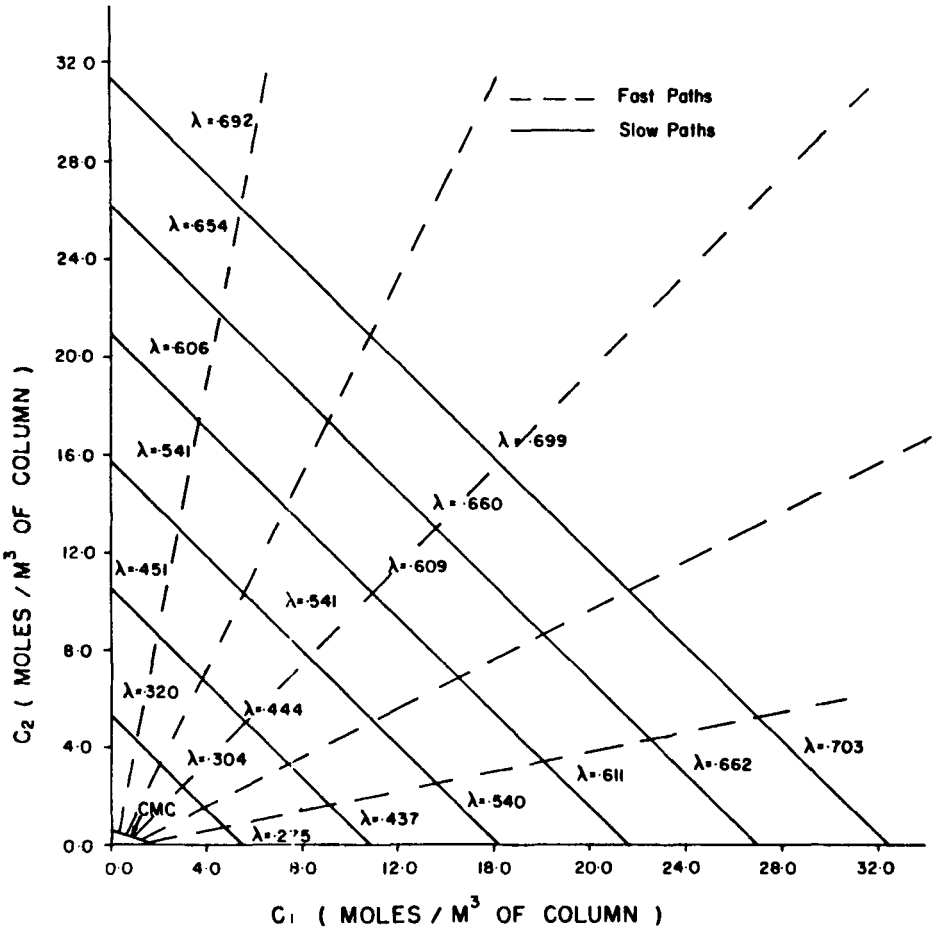

Figure 7. Composition path grid for higher concentrations.

details will not be repeated here.

The key step is the application of the coherence condition to construct a composition grid path (also called a hodograph). These composition paths are curves in the coordinate space of the dependent variables—here taken as the total (surfactant in both micelles and monomer) fluid phase composition, C_i—corresponding to variations that are coherent. For a system with given flow and equilibrium properties, a unique set of such paths can be constructed and then applied to any initial and boundary conditions. Figures 6 and 7 show the composition diagram constructed for the real surfactant isotherms described earlier in this paper.

These composition path diagrams for a real system may be compared with the topology of the idealized Trogus system composition path diagram previously published (Harwell et al., 1982). The most striking observation is the great similarity between the idealized system and the real system. Both contain the discontinuity at the CMC of the system and both have lines of constant adsorption as one family of composition paths (also called characteristic curves in the hodograph space) above the CMC. These lines of constant adsorption arise as a result of the phase separation model. Since this model is also used in the construction of the isotherms in the real system, these lines are again prominent features of the topology.

The contrasts between the systems are less dramatic. The CMC in the idealized system is curved; in the real system it is a straight line. This is simply because the idealized system did not include added electrolyte, whereas the real system is at 0.2 M NaCl. It also appears that the slow paths above the CMC in Figures 6 and 7 are straight lines. No analytical expression has been obtained for these curves, but it seems likely that their curvature or lack of curvature is also determined by the counterion concentration.

Another difference between the two systems are the eigenvelocities (called characteristic velocities in simple wave theory). Those in the idealized system are much higher both above and below the CMC than in the real system. This is an insignificant difference. The parameters for the idealized system were determined from fits of effluent profiles from a Berea sandstone core. Parmeter values for the present system are for surfactant adsorption on an α-alumina powder at a system pH below the point of zero charge of the oxide. Surfactant adsorption is much higher on the α-alumina than on the Berea and so the eigenvelocities are much lower in the present system. This has nothing to do with differences in models or with the form of the adsorption isotherms.

Note also that in the real system there is still an inversion curve (see Harwell et al., 1982) and that between the inversion curve and the CMC, eigenvelocities decrease along the slow paths in the direction of increasing C_1 and that above the inversion curve they increase along the slow paths in the direction of increasing C_1. In contrast to the idealized system of the previous paper, the exact position of the inversion curve in the real system is more difficult to determine by looking for a slow path with constant eigenvelocities. There are two reasons for this. One is the similarity between the surfactants in the real system—$3\phi C_9$ and $3\phi C_{10}$—differ only by one long-chain methyl group. The other is that the eigenvelocities are approximated by numerical differentiation. The combination of the very slowly changing eigenvelocities and the numerical approximations makes this an unsatisfactory method for locating the inversion curve accurately in the present case.

In summary, it must be said that the topology of the real and the idealized system above the CMC are qualitatively identical. Since the adsorption isotherms differ so drastically (Henry's law in one case, synergistic mixed aggregate formation on a heterogeneous surface in the other), this similarity must be attributed to the phenomenon of mixed micelle formation described by the pseudo phase separation model and plateau adsorption. These are the only aspects that the model of Harwell et al. (1982) and the model in this paper have in common, illustrating the extent to which mixed micelle formation and plateau adsorption determine the chromatographic behavior of aqueous surfactant mixtures.

The significant differences in idealized and real system topologies are below the CMC. Apart from the already discussed trivial observation that the magnitudes of the eigenvelocities are different, one significant observation is that the eigenvelocities are no longer constant along the paths and that the paths are curved. In the real system, spreading waves and shocks may arise from certain injection sequences; because the composition paths are curved, when shocks arise they may not follow the composition paths. Additionally, in the idealized system, wave/wave interactions were all noninterfering at concentrations below the CMC because there was no component interaction below the CMC. In the real system, complex surface interactions give rise to possible complex wave/wave interferences and extensive regions of noncoherence. Finally, the real system contains a discontinuity below the CMC, the mixture CAC. Below the CAC wave behavior is identical to that below the CMC in the idealized system: All composition paths are orthogonal, all eigenvelocities are constant along the paths, and all waves are noninterfering. The discontinuity in the solution space of the real system at the mixture CAC will be seen to have significant effects on chromatographic behavior.

Experimental Results

The experiments presented in this section were designed to demonstrate the major counterintuitive features of surfactant chromatographic behavior and to provide experimental support for conclusions based on the adsorption model. The theoretical curves in the following examples were not fit to the experimental results by use of an adjustable parameter; they are based entirely on the experimental parameters necessary to fit the isotherm model to the $3\phi C_9/3\phi C_{10}$ pure component adsorptions (Figures 3 and 4), on CMC data presented elsewhere (Harwell, 1983), and on estimates of the column void volume. The experiments were designed to demonstrate the following phenomena:

1. Formation of micelles enriched in the more strongly adsorbed component
2. Formation of micelles enriched in the less strongly adsorbed component
3. Existence of waves of unit velocity
4. Generation of multiple waves by the discontinuity at the CMC
5. Non-Henry's law behavior in the low concentration (below the CMC) region
6. Generation of a fast-moving low concentration wave by the discontinuity at the CAC
7. Effect of dispersion in wiping out any observable chromatographic separation in the present system at concentrations above the inversion curve.

Some of these phenomena will be present in more than one of the examples presented. Several of the phenomena are a consequence of the pseudophase separation model for monomer/micelle equilibrium and the plateau adsorption model. Hence, observation of unit velocity waves of overshoot of the more strongly adsorbed component, and of the generation of an additional chromatographic wave on eluting concentrations above the CMC constitutes dramatic confirmation of the applicability of both the pseudophase separation model of micelle formation and the plateau adsorption model to the system studied.

Case 1: Injection of $3\phi C_9$ABS Enriched Micellar Solution into Column Preequilibrated with a Micellar Solution. The injected composition and the composition with which the chromatographic column had been preequilibrated for this case are shown in Figure 8a, along with the predicted composition route. The original composition in the column is labeled composition O; the injected composition as composition I. The coherent path connecting compositions I and O follows a slow path from I to A, then a fast path from A to O. Eigenvelocities increase along the slow path from I to A (see Figure 8), indicating formation of a spreading wave; however, the velocities change very little. The wave of variation A/O is an indifferent wave of unit velocity; it corresponds to an increase in micelle concentration at constant monomer and adsorbed phase concentration and composition. Its existence in a real system depends on the applicability of the phase separation model. The predicted wave trajectories appear in Figure 8b and the observed composition route in Figure 8c. Note the close correspondence between the observed and predicted routes. The time-distance diagram of Figure 8b can be translated into an effluent history. The predicted and observed effluent histories are shown in Figure 8d. Taking as the midpoint of the leading wave the arithmetic average of the plateau values on either side of the wave, we arrive at a value of the plateau values on either side of the wave, $(3\phi C_{10}\text{ABS}) \approx 1.5^* (3\phi C_{10}\text{ABS})|_{\text{injected}}$ and so obtain $1/\Lambda_{A/O} =$

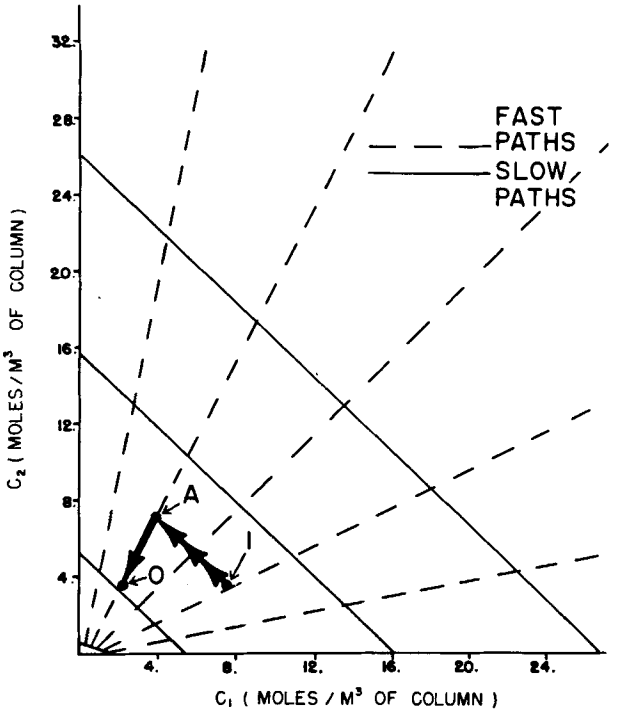

Figure 8a. Composition route for case 1.

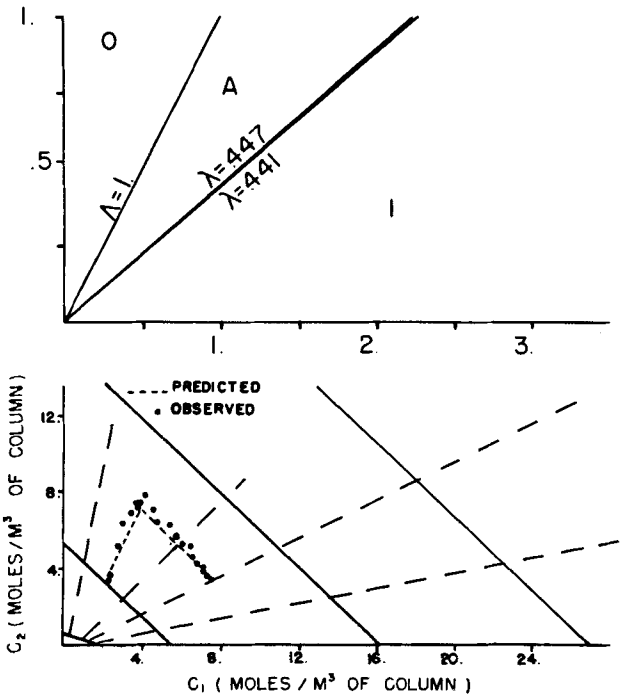

Figures 8b and 8c. Time-distance diagram for case 1; observed and predicted composition routes for case 1.

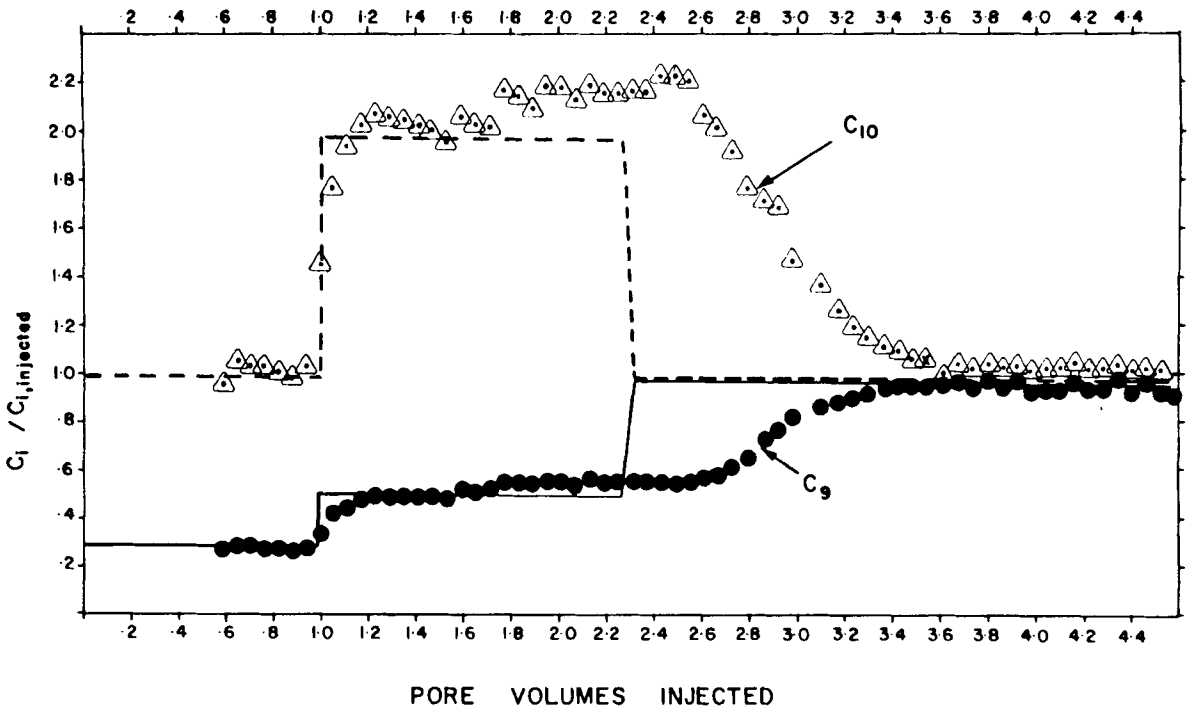

Figure 8d. Observed and predicted effluent profiles for case 1.

1.04 pore volumes, a normalized wave velocity ($\Lambda_{A/O}$) of 0.96 pore volumes traveled/pore volume injected. For the wave of variation A/O to have a velocity of approximately 96% of the bulk fluid velocity (predicted to be a unit velocity path), adsorption of the most strongly adsorbed component must have changed by only about ½%; the velocity of shocks and indifferent waves can be calculated from a mass balance across the wave

$$\Lambda = \frac{1}{1 + \dfrac{\Delta \overline{C}_i}{\Delta C_i}}$$

where $\Delta \overline{C}_i$ is the change in adsorption of i across the wave and ΔC is the change in solution concentration of i across the wave. Bear in mind that under the experimental conditions the α-alumina has only about ½ of bilayer coverage, while it has been shown that coverage could go up to complete bilayer formation (Scamehorn et al., 1982). Thus, adsorption changes from composition A to composition O by less than 0.5%, while total surfactant concentration goes from approximately 11 (mol/m^3 of column) at A to 5.6 (mol/m^3 of column) at O. To visualize this phenomenon, think of the solution at A as having the same monomer composition and micelles as at O but with more of these micelles. The wave A/O then represents the propagation of the same micelles already in the column. This is dramatic confirmation of the validity of both the phase separation model and the plateau adsorption model for the system being studied.

It is interesting to consider the counterintuitive behavior of the system observed in the experiments that is predicted by the model. Note that the injected and original concentrations have practically the same concentration of $3\phi C_{10}$ABS (3.61 mol/m^3 of column originally in the column and 3.60 mol/m^3 of column injected), whereas the injected concentration of $3\phi C_9$ABS is more than four times the original concentration of $3\phi C_9$ABS (7.57 mol/m^3 of column compared to 2.19 mol/m^3 of column). Despite the near constancy of the $3\phi C_{10}$ABS, the effluent history shows a pulse of $3\phi C_{10}$ABS over 2.5 pore volumes in size at nearly twice the injected concentration. This unexpected overshoot can be explained in terms of the plateau adsorption and phase separation models. Although the total concentration of $3\phi C_{10}$ABS is the same in the original and injected fluids, the monomer concentrations are not. The monomer concentration of the $3\phi C_{10}$ABS is predicted to be 0.407 mol/m^3 of column at composition O and 0.211 mol/m^3 of column at composition I. Correspondingly, composition A, which forms on injection of I against O, has the same monomer concentration and hence the same adsorption as O if the phase separation model is applicable. But since O has a higher concentration of $3\phi C_{10}$ABS monomers, the micelles at A are enriched with $3\phi C_{10}$ABS relative to the micelles at I. This is the cause of the otherwise difficult to explain pulse of $3\phi C_{10}$ABS in the effluent.

The second wave, the wave of variation I/A, arrives somewhat later than predicted. This indicates the change in adsorption from I to A is somewhat higher than predicted, since the values of concentrations correspond fairly well to the predicted values. One possible explanation of this is that the pH in the column differed somewhat from that at which the isotherm points were determined. Only small changes in pH in the area of pH 5 to 8 can result in very large changes in the total adsorption. Since very few hydrogen ions are needed to change the pH at pH 8, it may be very difficult to control the pH accurately in this region. Buffers were not used since the possible effects of their incorporation into both micelles and admicelles or the chromatographic behavior are unknown. Nevertheless, the results for this case clearly demonstrate the major conclusions of this study regarding the role of mixed micelle formation and plateau adsorption on surfactant chromatographic movement.

Case 2: Injection of $3\phi C_9$ABS Depleted Micellar Solution into a Column Preequilibrated with a Micellar Solution. Figure 9a contains plots of the injected composition I and the composition with which the column was preequilibrated (O) along with the predicted composition route and the composition of the plateau region that arises between compositions I and O. The coherent route from I to O follows a slow path from I to A, then a fast path from A to O. As before, the eigenvelocities along the path from A to O are constant at $\Lambda = 1$ and the wave of variation A/O is an indifferent wave. On the other hand, eigenvelocities decrease from I to A, so that the wave of variation I/A is a shock wave. The predicted trajectories of the waves appear in Figure 9b and the observed composition route in Figure 9c. Note again the close correspondence of the observed and predicted composition routes. The observed and predicted effluent histories are presented in Figure 9d. Taking the velocity of the first wave, the wave of variation O/A, as the velocity of the composition, which is the arithmetic average of the plateaus on either side of the wave, we obtain a velocity of $\Lambda = 0.98$ pore volumes traveled/pore volume injected. This tells us that the adsorption of $3\phi C_9$ABS changes by less than

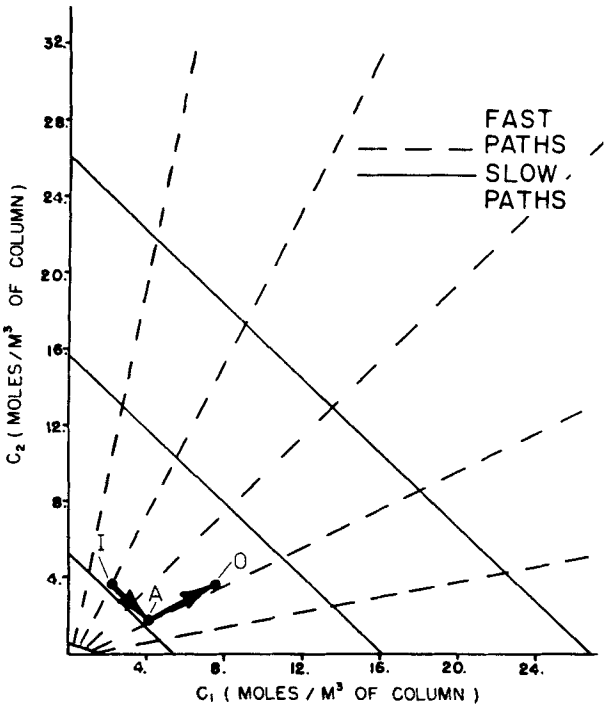

Figure 9a. Composition route for case 2.

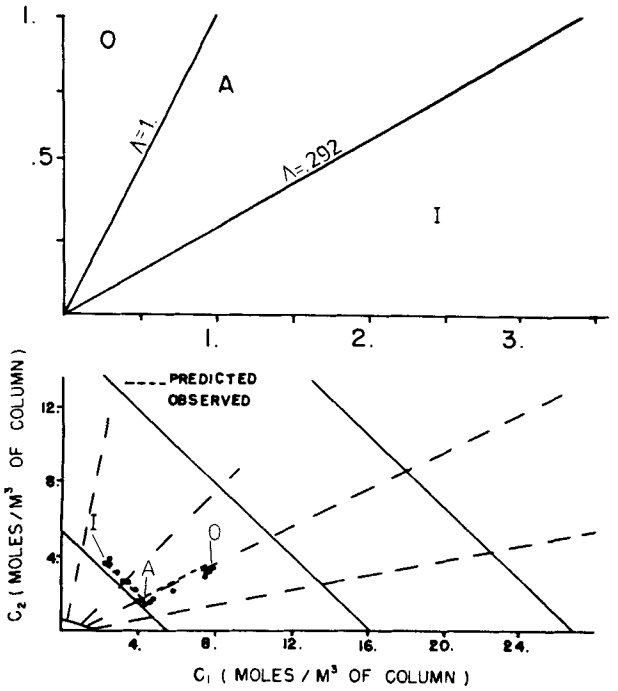

Figures 9b and 9c. Time-distance diagram for case 2; composition route for case 2.

0.2% from composition A to composition O, although the total fluid phase concentration changes from 4.09 to 7.57 moles/m^3 of column. This again is a dramatic demonstration of the validity of the phase separation and plateau adsorption models for this system and an illustration of the predicted effects of mixed micelle formation on the chromatographic behavior of these systems.

Note that in contrast to case 1, where using the same solutions we observed a large increase in the concentration of $3\phi C_{10}$ABS in the effluent, we now predict and observe a large decrease in $3\phi C_{10}$ABS concentration. Since the monomer concentration of $3\phi C_{10}$ABS is lower at composition O than at composition I, because of the preferential incorporation of the $3\phi C_{10}$ABS into the micellar pseudo phase at O, the micelles that form in equilibrium with the downstream monomers are depleted in $3\phi C_{10}$ABS. Thus, we observe a dip in $3\phi C_{10}$ABS concentration in the effluent.

Case 3: Injection of a Micelle Rich Slug into a Column Equilibrated with a Higher Monomer Concentration of the More Strongly Adsorbed Component ($3\phi C_{10}ABS$). In Figure 10a the

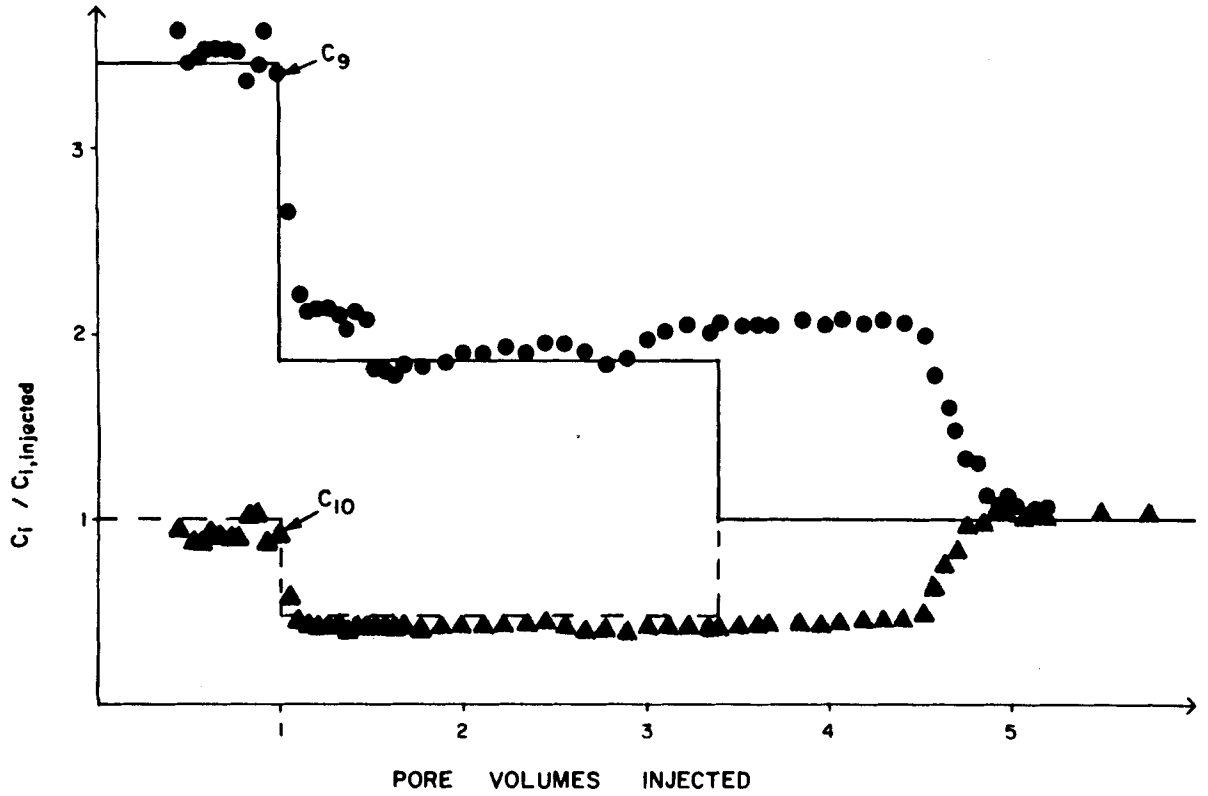

Figure 9d. Observed and predicted effluent profiles for case 2.

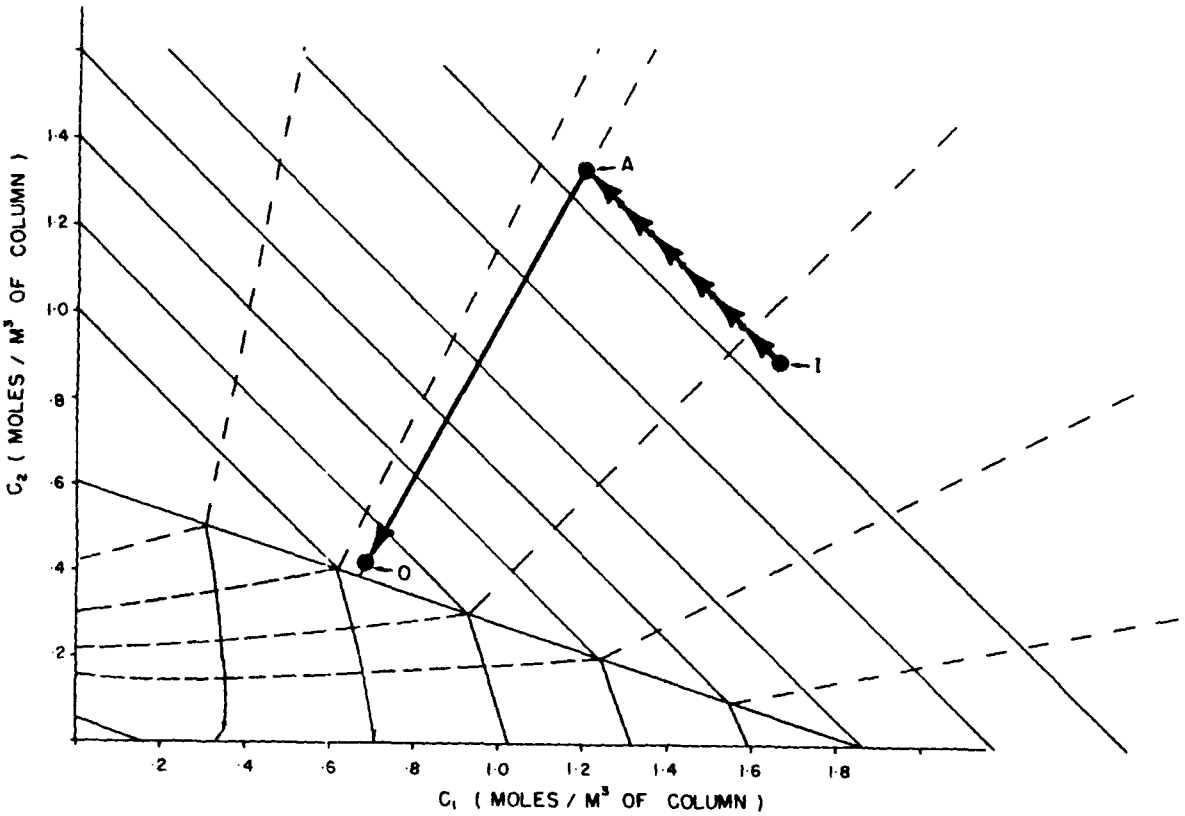

Figure 10a. Schematic of composition route for case 3.

alumina column has been preequilibrated with the solution indicated at point O. The solution to be injected is at point I. The original solution, O, is very near the CMC so that it has few micelles. While solution I is at a much higher concentration of $3\phi C_{10}$ (component 2), much of this $3\phi C_{10}$ is in the micelles, so that the $3\phi C_{10}$-monomer concentration is actually lower in solution I than in solution O. The predicted composition route in Figure 10a follows a slow path from I to A, then a unit velocity path from A to O. The eigenvelocities increase along the path from I to A, indicating formation of a spreading wave. The unit velocity wave is an indifferent wave. The predicted wave trajectories are shown in Figure 10b. The unit velocity wave quickly appears in the column effluent, followed nearly five pore volumes later by the spreading wave. The intermediate plateau region (where no waves are present) is at composition A from Figure 10a. The predicted and observed effluent profiles are presented in Figure 10c and the observed composition route in Figure 10d. From Figure 10d it can be seen that the observed composition route followed very closely the predicted route. Composition A corresponds to an increase in $3\phi C_{10}$ enriched micelles that are in equilibrium with the monomer ahead in the preflooded sections of the column. This is a consequence of both the phase separation and plateau adsorption models. In calculating the velocity of the leading wave (Figure 10c), take as the midpoint of the wave the point at which the concentration has reached the arithmetic average of the plateau regions behind and before the wave. This point is ($C_2/C_{2,\text{inj}} = 0.998$), which appears at 1.19 pore volumes, a normalized velocity of 0.84. Applying a mass balance across the wave front produces

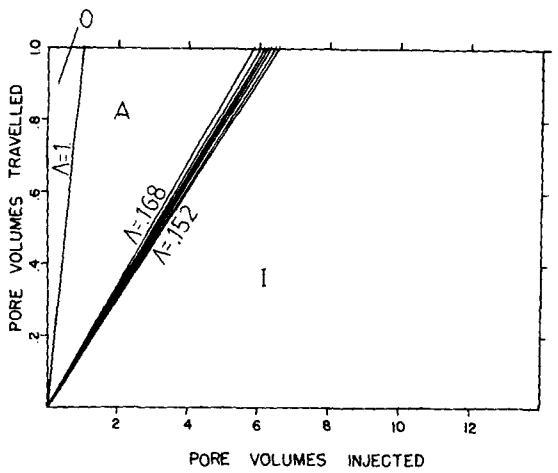

Figure 10b. Time-distance diagram for case 3.

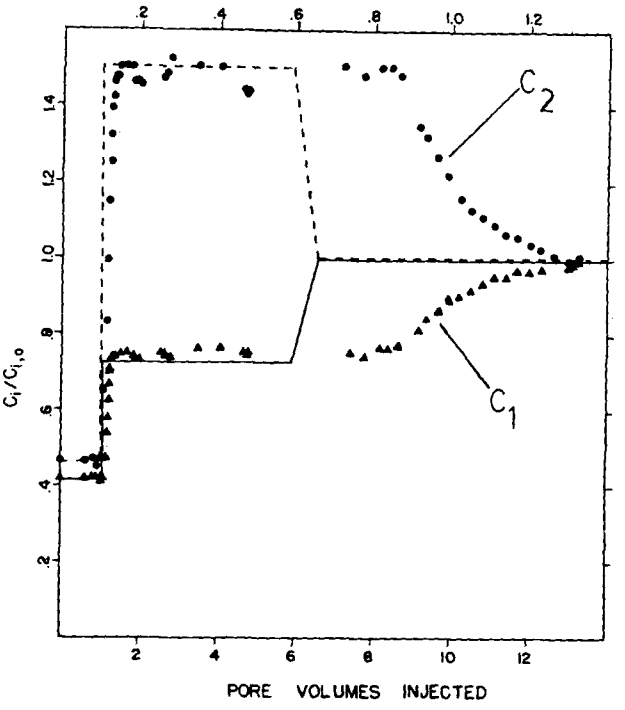

Figure 10c. Observed and predicted effluent histories for case 3.

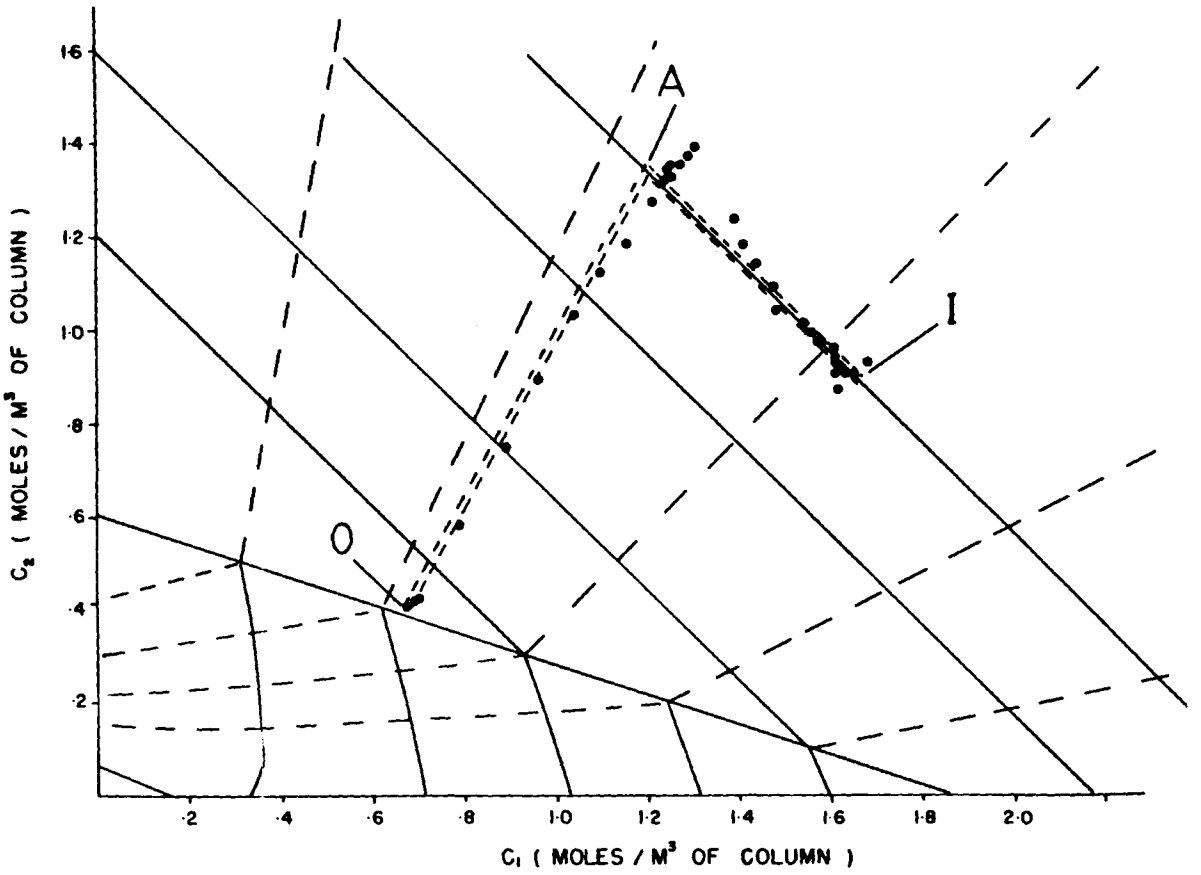

Figure 10d. Observed and predicted composition routes for case 3.

$$\Lambda = \frac{1}{\dfrac{1 + \Delta\overline{C}_2}{\Delta C_2}}$$

or

$$\Delta\overline{C}_2 = \frac{\Delta C_2(1 - \Lambda)}{\Lambda}$$

$$= 0.176 \text{ mol/m}^3 \text{ of column}$$

The amount of component 2 ($3\phi C_{10}$ABS) actually adsorbed is given by the theoretical isotherm as 8.7 moles/m^3 of column; thus the adsorption in going in from 0.415 moles of $3\phi C_{10}$/m^3 of column to 1.34 moles/m^3 of column is seen to change by only 2%:

$$\Delta\overline{C}_2 = \frac{0.176}{8.7} \times 100\% = 2\%$$

which is in excellent accordance with the plateau adsorption model.

The chromatographic behavior indicated in Figures 10c and 10d has possibly significant practical implications. Note that a very dilute surfactant preflood, just at the mixture CMC, at a higher concentration of monomers of the more surface active compound, results in overshoot of the more strongly surface active compound. A very large plateau zone is produced that is at a composition enriched in the more surface active compound. This presents the possibility of using the chromatographic behavior of surfactant mixtures to improve the oil recovery efficiency rather than reduce it. This possibility would, of course, have to be examined in light of the cost of equilibrating the reservoir or part of the reservoir with even a very dilute concentration of surfactant.

Case 4: Injection of a Composition Below the CMC. We have noted that below the CMC the composition paths for the real surfactant system are greatly different from those based on the idealized system. This experiment is designed to emphasize these differences. Correspondence between prediction and observation is much less satisfactory in this case; nevertheless, these results actually are a significant contribution to confirmation of the overall theory—comparison of predictions of chromatographic behavior in the idealized system of the previous paper and the real system of the present paper show considerable correspondence despite the tremendous differences in the actual adsorption models (as already discussed). Correspondence between predictions in the two models has been attributed to the assumption of the phase separation and the plateau adsorption models in both systems. In order for the observation of predictions based on these models in the real system to constitute a validation of the applicability of the models, it must be demonstrated that the correspondence is not because of the validity of the Henry's law model of the idealized system in the real system. Though it is actually sufficient to observe the isotherms of Figures 3, 4, and 5 to confirm this, it is still a necessary condition that the chromatographic behavior of the system below the CMC

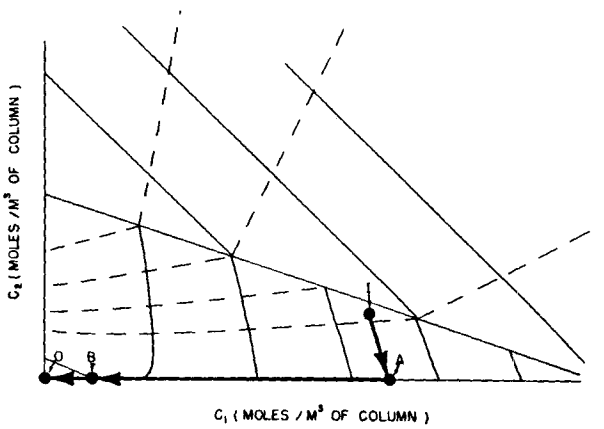

Figure 11a. Composition route for injection of infinite slug below CMC.

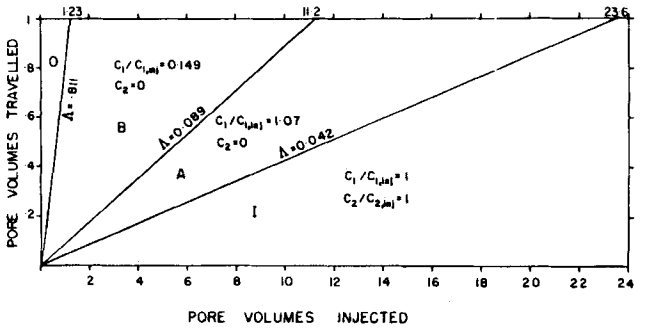

Figure 11b. Time-distance diagram for injection of infinite slug below CMC for case 5.

not be described by Henry's law behavior. Observation of non-Henry's law behavior in the real system below the CMC is then a confirmation that the results attributed to the validity of the phase separation and plateau adsorption models are not fortuitous results of the applicability of Henry's law to the real system. A typical example of Henry's law behavior is discussed fully in the previous paper; the key element of Henry's law behavior, however, is the formation of indifferent, noninterferring waves that result in eventual separation of slug components into separate pulses. The results reported here demonstate the influence of the discontinuity at the CAC and the complex interaction of the components on the surface.

The injected and original column conditions for the experiment are shown in Figure 11a. The composition route from *I* to *A* follows a slow path in a direction of decreasing eigenvalues (indicating shock formation) from composition *I* to *A*. From *A* the route follows a fast path to *B* in a direction of decreasing eigenvalues; at *B* the eigenvalue jumps at the discontinuity to a large value ($\Lambda = 0.811$), setting off an indifferent wave from *B* to *O*. The predicted wave trajectories are plotted in Figure 11b and the predicted and observed effluent histories in Figure 11c. The most significant feature in these plots is the appearance of component 1 ($3\phi C_9$ABS) at a very low value in the effluent very early; this is an experimental demonstration of a possible mechanism by which low equivalent weight surfactants appeared ahead of the incremental oil cut in the Bell Creek field test. It is present at 1.1 pore volumes, a velocity of $\Lambda = 0.91$, reasonably close to the predicted velocity of 0.81.

The departure of the observed route from the composition route can be qualitatively accounted for by considering the effects of dispersion. This can be done by drawing a mixing line between *I* and *O* on the composition path diagram and observing the resolution of this noncoherent path into a coherent one. At some point the processes resolving the paths into coherent ones become just balanced with the mixing effect of dispersion. This will be a stationary path. Lake and Hill (1978) have obtained quantitative solutions describing this balance for ion exchange processes. We simply note that the compositions take on a constant pattern where

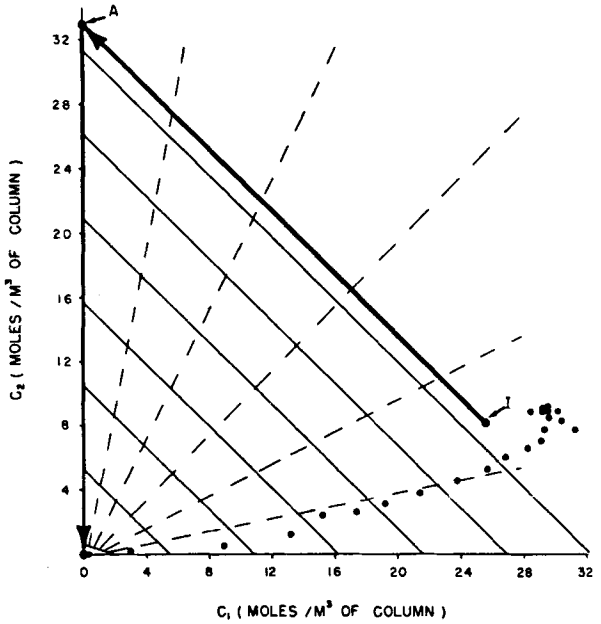

Figure 12a. Predicted and observed composition routes for case 6.

composition velocities and mixing are balanced. The shape of the observed route depends on the amount of dispersion, but it is possible to qualitatively arrive at the approximate shape of the observed route with very little difficulty.

The most important feature of this experiment is the rapidly moving low concentration waves of the less strongly adsorbed C_1. Not only does this demonstrate the non-Henry's law behavior below the CMC, but we believe that this wave will be a significant feature whenever a surfactant slug containing low equivalent weight components is injected into a porous medium initially devoid of surfactant.

Case 5: Injection of a Composition Above the Inversion Curve. Figure 12a contains the coherent and observed composition routes for the injection of composition *I*, a composition above the inversion curve, into a column devoid of surfactant, composition *O*. At first glance it would appear that there is no correspondence between the observed and predicted routes. This is not, however, the case. To see the relationship between prediction and experiment in Figure 12a, consider the wave trajectories plotted for this case in Figure 12b. Although a composition route can be constructed along coherent paths on the composition path grid, the trajectory plot (Figure 12b) shows the two coherent compositions to have velocities differing by only 0.002 of a pore volume traveled for each pore volume injected. It is apparent that there is a great deal of dispersion in the system under study. It should be exected then that there will be a great deal of mixing across the wave fronts between the original and injected compositions. This is even more evident in

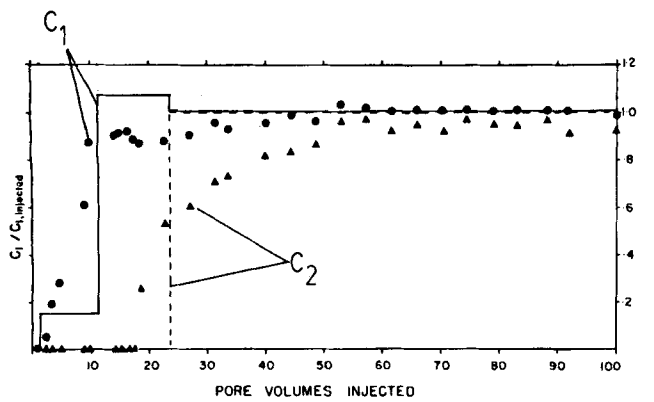

Figure 11c. Predicted and observed effluent histories for injection of composition below CMC for case 5.

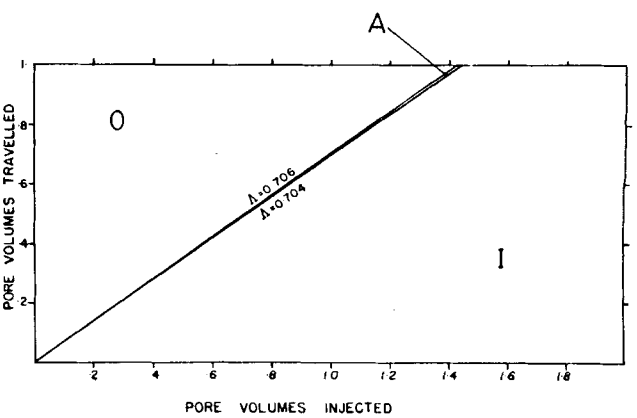

Figure 12b. Time-distance diagram for case 6.

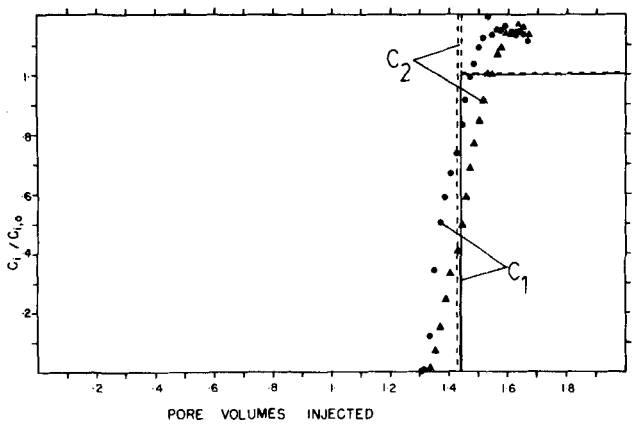

Figure 12c. Predicted and observed effluent histories for case 6.

Figure 12c. Ignoring momentarily the plotted exerimental data, note that the two predicted coherent waves would be separated by only thousandth of a pore volume in the effluent. Any mixing at all will destroy all evidence of the overshoot of the more strongly adsorbed component. This is, of course, exactly what is observed in Figure 12c. But what is the cause of the strange peak at the wave front? This phenomenon can be explained in terms of the wave attaining a constant or stationary pattern. Returning to Figure 12a, mixing across the wave fronts gives rise to compositions lying on a mixing line between *I* and *O*. This mixing generates compositions that are noncoherent, and the system begins to resolve these noncoherences along composition paths. However, this is prevented by continued mixing. The observed final pattern is attained by balancing coherence and mixing forces between the two concentrations *I* and *O*. One particularly interesting observation from this case is that dispersion and the tendency to form mixed micelles in equilibrium with downstream concentrations interact to practically eliminate any chromatographic separation at the slug front. We believe this to be a significant feature that would favor the use of small high concentration slugs that are at concentrations above the inversion curve rather than large low concentration ones.

Remarkably in this case even a small degree of dispersion will completely disrupt the composition path predicted by neglecting its effect. This is one of the few cases we know of in which small amounts of dispersion result in the complete disruption of a composition path. This would appear to be an important finding which merits further investigation. Additional results and more detailed discussions of the preceding cases may be found in Harwell (1983), along with development of the surfactant adsorption isotherm used in the theoretical predictions.

ACKNOWLEDGMENT

The research was supported by the U.S. Department of Energy, the Robert A. Welch Foundation, Amoco Production Co., Arco Oil and Gas Co., British Petroleum, Chevron Oil Field Research, Conoco, Inc., Dowell Division of Dow Chemical, Elf-Aquitaine, Exxon Production Research Co., GAF Corp., Getty Oil Co., Gulf Research and Development Co., Mobil Research and Development Co., Shell Development Co., Sun Production Co., Tenneco Oil Co., Texaco U.S.A., TOTAL, Union Oil Co., and Witco Chemical Corp.

Schechter holds the Dula and Ernest Cockrell, Sr., Chair (in Chemical and Petroleum Engineering).

NOTATION

A_i = empirical constant for phase separation model for component i (Eq. 3)
c_d = total monomer concentration i equals mixture CMC, mol/m^3 of solution
c_i = total concentration of i in solution, monomers plus micelles, mol/m^3 of solution
$c_{i,d}$ = concentration of dispersed monomers of component i, mol/m^3 of solution
$c_{i,m}$ = concentration of component i aggregated into micelles, mol/m^3 of solution
c_i^* = pure component CMC of i at mixture counterion concentration, mol/m^3 of solution
c_s = concentration of added electrolyte, mol/m^3 of solution
q_i = concentration of i adsorbed, mol/kg of adsorbate
C_i = total concentration of i in solution, micelle plus monomer, mol/m^3 of column
$C_{i,d}$ = concentration of dispersed i monomers, mol/m^3 of solution
$C_{i,m}$ = concentration of i in micellar form, mol/m^3 of column
$C_{i,o}$ = initial value of solution concentration of i in column, mol/m^3 of column
$C_{i,in}$ = concentration of i in injected solution, mol/m^3 of column
$C_{i,T}$ = total concentration of i per unit volume of column, solution plus adsorbed, mol/m^3 of column
C_i^* = pure component CMC of i at mixture counterion concentration, moles of i/m^3 of column
$\overline{C}_i$ = concentration of i adsorbed, mol/m^3 of column
CAC = critical admicelle concentration: concentration of surfactants at which surfactant aggregates begin to form on adsorbent, mol/m^3; analogous to HMC, hemimicelle concentration, used by some other authors (Somasundaran and Fuerstenau, 1966)
CMC = critical micelle concentration: solution surfactant concentration at which micellar aggregates begin to form in solution, mol/m^3
$K_{g,i}$ = empirical constant for phase separation model for component i (Eq. 3)
t = time, s
V = superficial fluid velocity of solution through column, m/s
z = distance from column inlet, m

Greek Letters

ΔC_i = change in the solution concentration of i across a shock wave, mol/m^3 of column
$\Delta\overline{C}_i$ = change in the adsorbed concentration of i across a shock wave, mol/m^3 of column
λ = an eigenvelocity in coherence theory (Helfferich and Klein, 1970); a characteristic velocity in simple wave theory (Aris and Amundson, 1973)
Λ = normalized velocity of a shock wave, pore volumes traveled/pore volume injected; $\Lambda = V_c/V$, where V is the superficial fluid velocity (m/s) and V_c is the velocity of the shock wave (m/s)
ϕ = column void fraction, m^3 of solution/m^3 of column
$\hat{\rho}_s$ = adsorbent density, kg/m^3 of adsorbate

LITERATURE CITED

Aho, G. E., and J. Bush, "Results of the Bell Creek Unit A Micellar-Polymer Pilot," SPE 11195, Annual Tech. Conf. and Exhibition of the Soc. of Petrol. Engineers, New Orleans (Sept. 26–29, 19182).

Ananthapadmanabhan, K. P., and P. Somasundaran, "Mechanism for Adsorption Maximum and Hysteresis in a Sodium Dodecylbenzenesulfonate/Kaolinite System," *Colloids and Surfaces*, **77**, 105 (1983).

Aris, R., and N. R. Amundson, *Mathematical Methods in Chemical Engineering*, Prentice-Hall, Englewood Cliffs, NJ, 268 (1973).

Doe, P. H., et al., "The Low Interfacial Tension Behavior of Pure Sodium Alkylbenzene Sulfonates," *Chem. Soc.*, **54**, 570 (1977).

Harwell, J. H., "Surfactant Adsorption and Chromatographic Movement with Application in Enhanced Oil Recovery," Ph.D. Dissertation, University of Texas at Austin (May, 1983).

Harwell, J. H., F. G. Helfferich, and R. S. Schechter, "Effects of Micelle Formation on Chromatographic Movement of Surfactant Mixtures," *AIChE J.*, **28**(3), 448 (1982).

Helfferich, F. G., and G. Klein, *Multicomponent Chromatography: Theory of Interference*, Marcel Dekker, New York, 52 (1970).
Holm, L. W., "Design, Performance and Evaluation of the Uniflood Micellar-Polymer Process-Bell Creek Field," SPE 11196, Annual Tech. Conf. and Exhibition of the Soc. of Petrol. Engineers, New Orleans (Sept. 26–29, 1982).
Lake, L. W., and H. J. Hill, "Cation Exchange in Chemical Flooding: Part 3—Experimental," *Soc. Petrol. Engrs. J.*, **18**(6), 445 (1978).
Lake, L. W., and G. W. Pope, "Status of Micellar-Polymer Field Tests," *Petrol. Eng. Int.*, **51**(13), 38 (1979).
Mysels, K. J., and R. J. Otter, "Thermodynamic Aspects of Mixed Micelles—Application of an Empirically Established Equilibrium," *J. Colloid Sci.*, **16**, 474 (1961).
Scamehorn, J. F., R. S. Schechter, and W. H. Wade, "Adsorption of Surfactants on Mineral Oxide Surfaces from Aqueous Solutions. I. Isomerically Pure Anionic Surfactants," *J. Colloid and Interface Sci.*, **85**(2), 463 (1982a); "II. Binary Mixture of Anionic Surfactants," *J. Colloid and Interface Sci.*, **85**(2), 476 (1982b).
Shinoda, K., *Colloidal Surfactant*, Academic Press, New York, 65 (1963).
Somasundaran, P., and D. W. Fuerstenau, "Mechanisms of Alkyl Sulfonate Adsorption at the Alumina-Water Interface," *J. Phys. Chem.*, **70**(1), 90 (1966).
Trogus, F. J., et al., "Adsorption of Mixed Surfactant Systems," *J. Petrol. Technol.*, **31**, 769 (1979a).
Trogus, F. J., R. S. Schechter, and W. H. Wade, "A New Interpretation of Adsorption Maxima and Minima," *J. Colloid and Interface Sci.*, **70**, 293 (1979b).

Manuscript received Aug. 15, 1983; revision received Jan. 20, 1984, and accepted Jan. 28.

Synthesis of Control Structures by Singular Value Analysis: Dynamic Measures of Sensitivity and Interaction

HENRY LAU, JESÚS ALVAREZ, and K. F. JENSEN

Department of Chemical Engineering and Materials Science University of Minnesota Minneapolis, MN 55455

A strategy for synthesizing regulatory control structures is developed within the framework provided by singular value decomposition (SVD). Quantitative measures of interaction and sensitivity for the nodes, as well as for the entire system, are established with this method. The approach enables analysis of the control structure over a range of frequencies which are of practical importance for a particular processing unit, thus insuring that both static and dynamic effects are encompassed. In addition, this method allows the designer to identify the modeling aspects which are important in determining the performance of the synthesized control structures. A series of examples, presented in order of increasing complexity, demonstrate the usefulness and versatility of this procedure. The technique is implemented as an interactive computer package.

SCOPE

The design of a regulatory control structure for a chemical process is one of the most challenging tasks confronting the control engineer. It has been suggested (Foss, 1973; Lee and Weekman, 1976; Stephanopoulos, 1982) that the relevant problem in chemical engineering process control is not the development of more sophisticated algorithms, but rather the establishment of a structural framework for selecting the manipulated and measured variables and linking them appropriately. In industrial practice the loop pairing is often based on the experience and intuition of the process control engineer. Many techniques have been proposed to rationalize the selection of loop pairings. Bristol's relative gain array (Bristol, 1966), which indicates the proper pairings for minimum static interactions among control loops, has been popular because it is easy to use and only requires knowledge of steady-state process gains. However, stronger interactions may exist during transients, and these may dictate a different control structure than that predicted by the static analysis (Tung and Edgar, 1977). Consequently, measures of process interaction have been proposed which include dynamic effects (Witcher and McAvoy, 1977; Tung and Edgar, 1977; Gagnepain and Seborg, 1982). However, the simple criteria may not be as reliable as computer-aided design packages such as the inverse Nyquist array or the characteristic loci (Ray, 1982).

In this paper we describe a control structure synthesis strategy based on the singular values (also known as principal gains) of the open-loop transfer function. The magnitude of the singular values measures the sensitivity of multiinput/multioutput (MIMO) systems in the same manner as the amplitude ratio is employed in single-input/single-output (SISO) systems. In addition, new and quantitative measures of interactions among control loops are developed. In order to encompass both static and dynamic features, the analysis is carried out over a range of frequencies of practical significance for a given process. Moreover, the analysis is combined with the design of structural compensators which minimize interactions among control loops over a range of frequencies characteristic of major process disturbances. The methodology is illustrated with examples, and particular emphasis is placed on the structural and physical interpretations of the process analysis and of the resulting control structure.

Correspondence concerning this paper should be addressed to K. F. Jensen.
Henry Lau is presently at Shell Development Company, Westhollow Research Center, Houston, TX 77001.
Jesús Alvarez is presently at Universidad Autonoma Metropolitana (Iztapalapa), Departmento de Ingenieria, 09340 Mexico D.F.